

# Super Critical Water-Cooled Nuclear Reactors (SCWRs) Thermodynamic Cycle Options and Thermal Aspects of Pressure-Channel Design

**M. Naidin, I. Pioro, R. Duffey\*, S. Mokry, L. Grande, B. Villamere,  
L. Allison, A. Rodriguez-Prado, S. Mikhael and K. Chophla**

University of Ontario Institute of Technology  
Faculty of Energy Systems and Nuclear Science  
2000 Simcoe Street North, Oshawa, Ontario, L1H 7K4, Canada  
[maria.naidin@mycampus.uoit.ca](mailto:maria.naidin@mycampus.uoit.ca); [igor.pioro@uoit.ca](mailto:igor.pioro@uoit.ca); [sarah.mokry@mycampus.uoit.ca](mailto:sarah.mokry@mycampus.uoit.ca);  
[lisa.grande@xplornet.com](mailto:lisa.grande@xplornet.com)

\*Chalk River Laboratories, Atomic Energy of Canada Limited  
Chalk River, Ontario, K0J 1J0 Canada  
[duffeyr@aecl.ca](mailto:duffeyr@aecl.ca)

**Abstract.** Research activities are currently underway worldwide to develop Generation IV nuclear reactor concepts with the objective of improving thermal efficiency and increasing economic competitiveness of Generation IV Nuclear Power Plants (NPPs) compared to modern thermal power plants. The SuperCritical Water-cooled Reactor (SCWR) concept is one of six Generation IV options chosen for further investigation and development in many countries, including Canada.

Water-cooled reactors operating at subcritical pressures (7 – 16 MPa) have provided significant electricity production for the past 50 years. However, the thermal efficiency of current NPPs is not very high (30 – 35%). As such, more competitive designs with higher thermal efficiencies, which will be close to that of modern supercritical thermal power plants (45 – 50%), need to be developed and implemented.

Previous studies have shown that direct cycles, with no-reheat and single-reheat configurations are the best choices for a SCWR concept. There are a few technical challenges associated with the no-reheat and single-reheat SCW NPP configurations. The single-reheat cycle requires nuclear steam-reheat, thus increasing the complexity of the reactor core design. Conversely, the major technical challenge associated with a SC no-reheat turbine is high moisture content in the low-pressure turbine exhaust.

The SCWR-core concept investigated in this paper is based on a generic pressure-tube (pressure-channel) reactor with a 43-element bundle string cooled with supercritical water. The considered 1200-MW<sub>el</sub> reactor has the following operating parameters: pressure of 25 MPa and reactor inlet/outlet temperatures of 350°C/625°C.

Previous studies have shown that if uranium dioxide (UO<sub>2</sub>) is used the fuel centerline temperature might exceed the conservatively established industry accepted limit of 1850°C. Therefore, this paper investigates a possibility of using uranium carbide (UC), uranium nitride (UN) and uranium dicarbide (UC<sub>2</sub>) as SCWR fuels since they have significantly higher thermal conductivities when compared to conventional nuclear fuels such as UO<sub>2</sub>, MOX and ThO<sub>2</sub>.

Also, important thermalhydraulic parameters such as a bulk-fluid temperature, heat transfer coefficient, outer-sheath and fuel centerline temperatures have been calculated along the heated bundle-string length at non-uniform cosine-based Axial Heat Flux Profiles (AHFPs).

In addition, a new heat-transfer correlation for supercritical water flowing in vertical circular bare tubes was proposed. This correlation can be used for a preliminary conservative estimation of heat transfer coefficients in SCWRs as bundle correlations have not been yet developed.

## 1. INTRODUCTION

Currently, there are a number of Generation IV SCWR concepts under development worldwide [1]. The main objectives for developing and utilizing SCWRs are: 1) Increase thermal efficiency of current NPPs from 30 – 35% to approximately 45 – 50%, and 2) Decrease capital and operational costs and, in doing so, decrease electrical-energy costs.

SCW NPPs will have much higher operating parameters compared to current NPPs (i.e., pressures of about 25 MPa and outlet temperatures up to 625°C) (Figure 1). Additionally, SCWRs will have a simplified flow circuit in which steam generators, steam dryers, steam separators, etc., will be eliminated. Furthermore, SCWRs operating at higher temperatures can facilitate an economical production of hydrogen through thermochemical cycles or direct high-temperature electrolysis [2, 3].

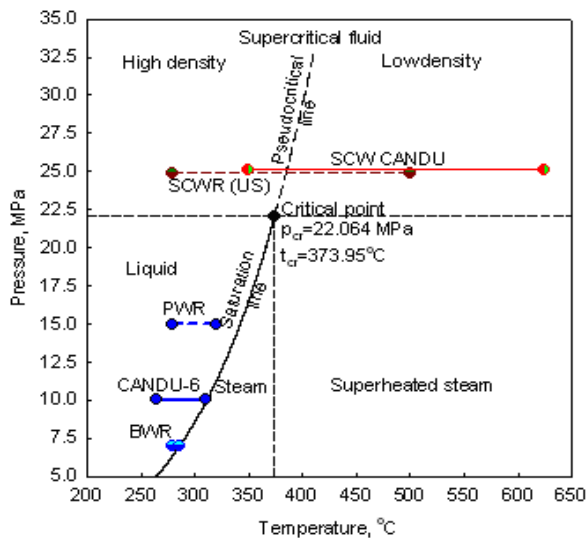


Fig. 1. Pressure-temperature diagram of water for typical operating conditions of SCWRs, PWRs, CANDU-6 reactors and BWRs.

The SCWR concepts [1, 4–6] follow two main types: (a) A large reactor pressure vessel (PV) analogous to conventional Light Water Reactors (LWRs); or (b) Distributed pressure tubes (PTs) or pressure channels analogous to conventional Heavy Water Reactors (HWRs). Within these two main classes, PT reactors are more flexible to flow, flux and density changes than PV reactors. This makes it possible to use the experimentally confirmed, better solutions developed for these reactors. The main ones are fuel re-loading and channel-specific flow-rate adjustments or regulations. A design whose basic element is a channel, which carries a high pressure, has an inherent advantage of greater safety than large vessel structures at supercritical pressures.

To decrease significantly the development costs of a SCW NPP and to increase its reliability, it should be determined whether

SCW NPPs can be designed with a steam-cycle arrangement similar to that of SC fossil-fired power plants (including their SC-turbine technology), which have been used extensively at existing thermal power plants for the last 50 years.

## 2. GENERAL CONSIDERATIONS REGARDING SCW NPP CYCLE

### 2.1 Review of SC Turbines

SC-“steam” turbines of medium and large capacities (450 – 1200 MW<sub>el</sub>) [5] have been used very successfully at many fossil power plants worldwide for more than fifty years. Their steam-cycle thermal efficiencies have reached nearly 54%, which is equivalent to a net-plant efficiency of approximately 40 – 43% on a Higher-Heating Value (HHV) basis. Table 1 lists selected current and upcoming SC turbines manufactured by Hitachi for reference purposes.

Table 1. Major Parameters of Selected Current and Upcoming Hitachi SC Plants [7].

| First Year of Operation | Power Rating, MW <sub>el</sub> | $P$ , MPa | $T_{\text{main}} / T_{\text{reheat}}$ , °C |
|-------------------------|--------------------------------|-----------|--|
| 2011                    | 495                            | 24.6      | 566/566                                    |
| 2010                    | 677                            | 25.5      | 566/566                                    |
|                         | 809                            | 25.4      | 579/579                                    |
|                         | 790                            | 26.4      | 600/620                                    |
| 2009                    | 677                            | 25.5      | 566/566                                    |
|                         | 600                            | 25.5      | 600/620                                    |
| 2008                    | 1000                           | 24.9      | 600/600                                    |
|                         | 870                            | 24.7      | 566/593                                    |
|                         | 870                            | 24.7      | 566/593                                    |
| 2007                    | 1000                           | 24.9      | 600/600                                    |
|                         | 870                            | 25.3      | 566/593                                    |

An analysis of SC-turbine data [5] showed that:

- The vast majority of the modern and upcoming SC turbines are single-reheat-cycle turbines;
- Major “steam” inlet parameters of these turbines are: The main or primary SC “steam” –  $P = 24 - 25$  MPa and  $T = 540 - 600$ °C; and the reheat or secondary subcritical-pressure steam –  $P = 3 - 5$  MPa and  $T = 540 - 620$ °C.
- Usually, the main “steam” and reheat-steam temperatures are the same or very close (for example, 566/566°C; 579/579°C; 600/600°C; 566/593°C; 600/620°C).
- Only very few double-reheat-cycle turbines were manufactured so far. The market demand for double-reheat turbines disappeared due to economic reasons after the first few units were built.

## 2.2 Direct, Indirect and Dual Cycle Options

Since the “steam” parameters of a SCW NPP are much higher than those of current NPPs, several conceptual designs have been investigated to determine the optimum configuration. As such, direct, indirect and dual cycles have been considered [3, 5–10].

In a direct cycle, SC “steam” from the nuclear reactor is fed directly to a SC turbine. This concept eliminates the need for complex and expensive equipment such as steam generators. From a thermodynamic perspective, this allows for high steam pressures and temperatures, and results in the highest cycle efficiency for the given parameters.

The indirect and dual cycles utilize heat exchangers (steam generators) to transfer heat from the reactor coolant to the turbine. The indirect cycle has the safety benefit of containing the potential radioactive particles inside the primary coolant. However, the heat-transfer process through heat exchangers reduces the maximum temperature of the secondary loop coolant, thus lowering the efficiency of the cycle.

Since increasing the thermal efficiency is one of the main objectives in the development of SCW NPPs, direct cycles are further investigated in this paper.

## 2.3 Reheating Options for SCW NPP

A preliminary investigation of SCW NPP reheat options [10] revealed the following:

- The no-reheat cycle offers a simplified SCW NPP layout, contributing to lower capital costs. However, the efficiency of this cycle is the lowest of all the considered configurations.

- The single-reheat cycle has the advantage of higher thermal efficiency (compared to that of the no-reheat cycle) and reduced development costs due to a wide variety of single-reheat SC turbines manufactured by companies worldwide. The major disadvantage is an increased design complexity associated with the introduction of Steam-ReHeat (SRH) channels to the reactor core.
- While the double-reheat cycle has the highest thermal efficiency, it was deemed that the complicated nuclear-steam reheat configuration would significantly increase the design and construction costs of such a facility.
- As such, configurations based on the no-reheat and single-reheat cycles were chosen for the analysis in this paper.

## ***2.4 Regenerative Cycle***

Another way of increasing the average temperature during heat addition is to increase the temperature of feedwater entering the SCWR. In practice, regeneration is accomplished through feedwater heaters. Steam extracted from the turbine at various points is used to heat the feedwater to the desired temperature. The regeneration process does not only improve the cycle efficiency, but also improves the quality of the feedwater system by removing air and other non-condensable gases.

As previously mentioned, the reactor inlet temperature is approximately 350°C. It is obvious that a regenerative cycle needs to be implemented to increase the feedwater temperature from the condenser outlet (about 40°C) to the reactor inlet conditions (350°C).

## ***2.5 Assumptions and Simplifications***

For the purpose of completing the thermal analysis of the proposed cycles, several assumptions were considered, as follows:

- Gland-Steam System and auxiliary-steam consumers were neglected.
- Performance losses associated with mechanical equipment, turbine-packing leakage, generator and piping-pressure drops were also neglected.

System parameters such as mass flowrates, power outputs, etc., are calculated for an NPP power output of 1200 MW<sub>el</sub>. It is assumed that all processes are steady-state and steady-flow with negligible potential and kinetic effects and no chemical reactions. Also, heat and work transfer to the system are considered positive values.

## **3. SCW NPP CYCLES DESCRIPTION**

### ***3.1 Single-Reheat Cycles System Description***

The proposed cycle layouts for a SCW NPP with a single-reheat option are shown in Figures 2 and 3 (Cycles A and B). As per the previous sections, the cycles have direct single-reheat, regenerative configurations. As such, the SC “steam” exiting the reactor is expanded through a single-flow HP turbine.

As shown in Figure 2, for Cycle A the steam is sent back to the reheater (SRH channels inside the reactor), where the temperature is raised to superheated conditions. Furthermore, the subcritical-pressure superheated steam (SHS) is expanded in the Intermediate-Pressure (IP) turbine and transferred, through a cross-over pipe, to the Low-Pressure (LP) turbines. Since the volume of the steam at the exhaust of the IP turbine is quite high, two LP turbines are being utilized. In Figure 2, the turbine-generator arrangement is a cross-compound: the High-Pressure (HP) and IP turbines are located on the same shaft, while the LP turbines are located on a separate shaft.

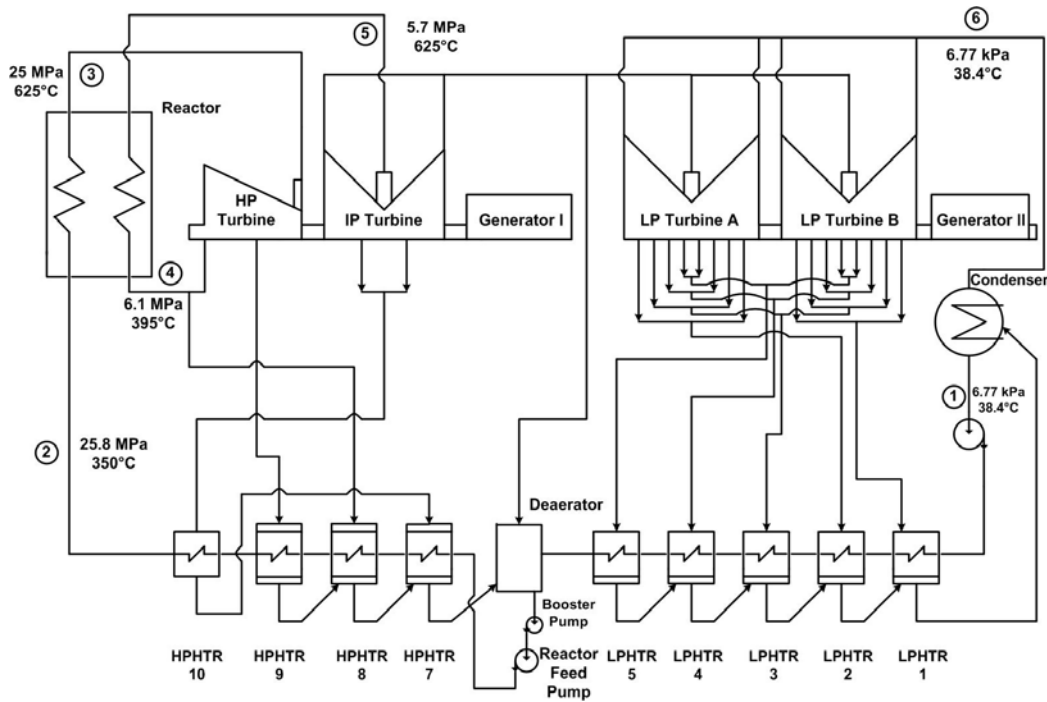


Fig. 2. Single-Reheat Cycle A for SCW NPP [7].

Cycle B, shown in Figure 3, follows a slightly different arrangement. As such, the steam expanded in the HP turbine is sent to the IP turbine where it expands to saturated conditions (approximately 98% steam quality). Furthermore, the steam is passed through a Moisture-Separator-Reheater (MSR) unit that contains one stage of moisture separation and two stages of reheat. From here, superheated steam exiting the MSR unit is sent to the inlet of the LP turbines where it is expanded to saturated conditions. The steam is exhausted from the turbine to the condenser, suffering exhaust losses, which depend on the exhaust area and steam velocity. The saturated steam undergoes a phase change and is condensed at a constant pressure and temperature by a cooling medium inside the condenser. The Condensate Extraction Pump (CEP) is taking its suction from the condenser outlet. It pumps the condensate from the hotwell through a series of LP-feedwater heaters (LP HTR 1 to 5 for Cycle A, LP HTR 1 to 4 for Cycle B) to the deaerator. The feedwater temperature differentials across the LP heaters are assumed approximately the same. The LP heaters are tube-in-shell, closed-type heat exchangers. On the steam side, they contain condensing and subcooling zones.

The deaerator is an open-type feedwater heater, where the feedwater, extraction steam and drains of the HP heaters come into a direct contact. The feedwater is heated (at constant pressure) to the saturation temperature, and leaves the deaerator as saturated liquid. The Reactor Feedwater Pump (RFP) takes its suction from the deaerator and raises the feedwater pressure to the required value at the reactor inlet.

Furthermore, the feedwater is passed through 3 HP heaters (HP HTR 7 to 9) and a topping de-superheater (HP HTR 10) for the configuration described in Cycle A. Similarly, the feedwater passes through 4 HP heaters (HP HTR 6 to HP HTR 9) in the case of Cycle B. The HP heaters are tube-in-shell, closed-type heat exchangers with de-superheating, condensing and subcooling zones.

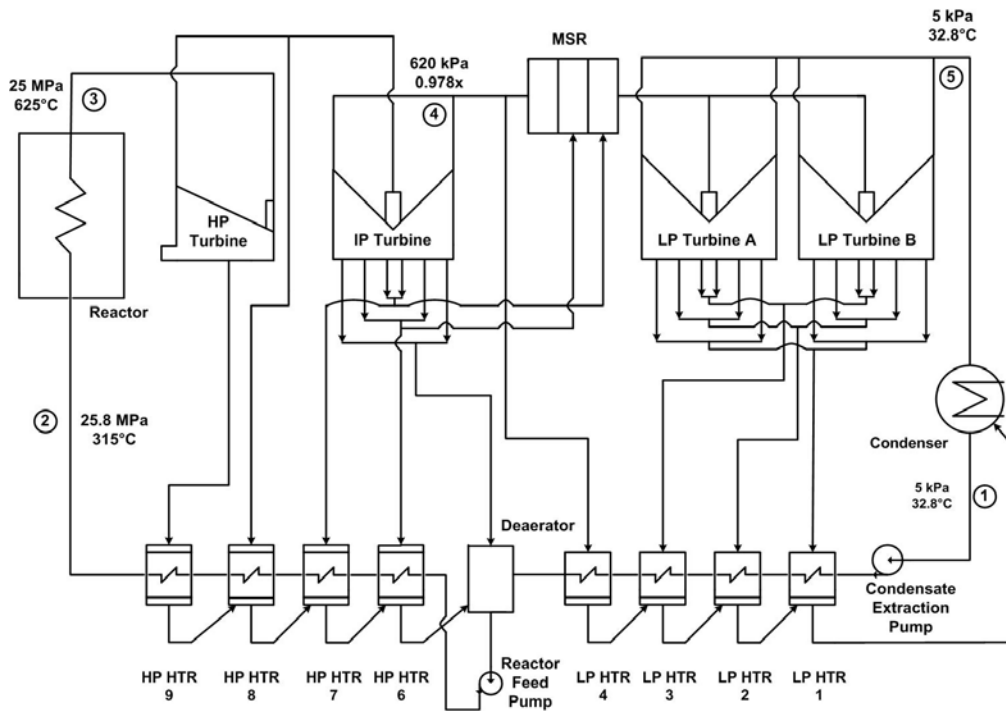


Fig. 3. Single-Reheat Cycle B for SCW NPP [5]

### 3.2 No-Reheat Cycles System Description

The single-reheat cycle introduces nuclear SRH channels, thus increasing the complexity of the reactor core design. Although preliminary results show that the thermal efficiency of the no-reheat cycle is approximately 1 – 2% lower than that of single-reheat cycles, the less complex core configuration might prove to be a major factor when selecting the most suitable design. In conclusion, it is worth analyzing the possibility of a no-reheat SCW NPP cycle such as the one proposed in this paper.

The proposed no-reheat SCW NPP cycle consists of five LP-feedwater heaters, one deaerator, three HP-feedwater heaters and one topping de-superheater (see Figure 4). The cycle has a direct, no-reheat, regenerative configuration. As such, the SC “steam” exiting the reactor is expanded through a double-flow HP turbine to superheated conditions. Since the volume of the steam at the exhaust of the HP turbine is quite high, two IP/LP turbines are being utilized. Furthermore, the steam is exhausted from the IP/LP turbine to the condenser. The saturated steam undergoes a phase change and is condensed at constant pressure and temperature by a cooling medium inside a condenser.

CEP is taking its suction from the condenser hotwell. It pumps the condensate through a series of five LP-feedwater heaters (LP HTR 1 to 5) to the deaerator. The feedwater is heated at constant pressure, and leaves the deaerator as saturated liquid. RFP takes its suction from the deaerator and raises the feedwater pressure to the required value at the reactor inlet (25 MPa). Furthermore, the feedwater is passed through three HP heaters (HP HTR 7 to 9) and a topping de-superheater (HP HTR 10).

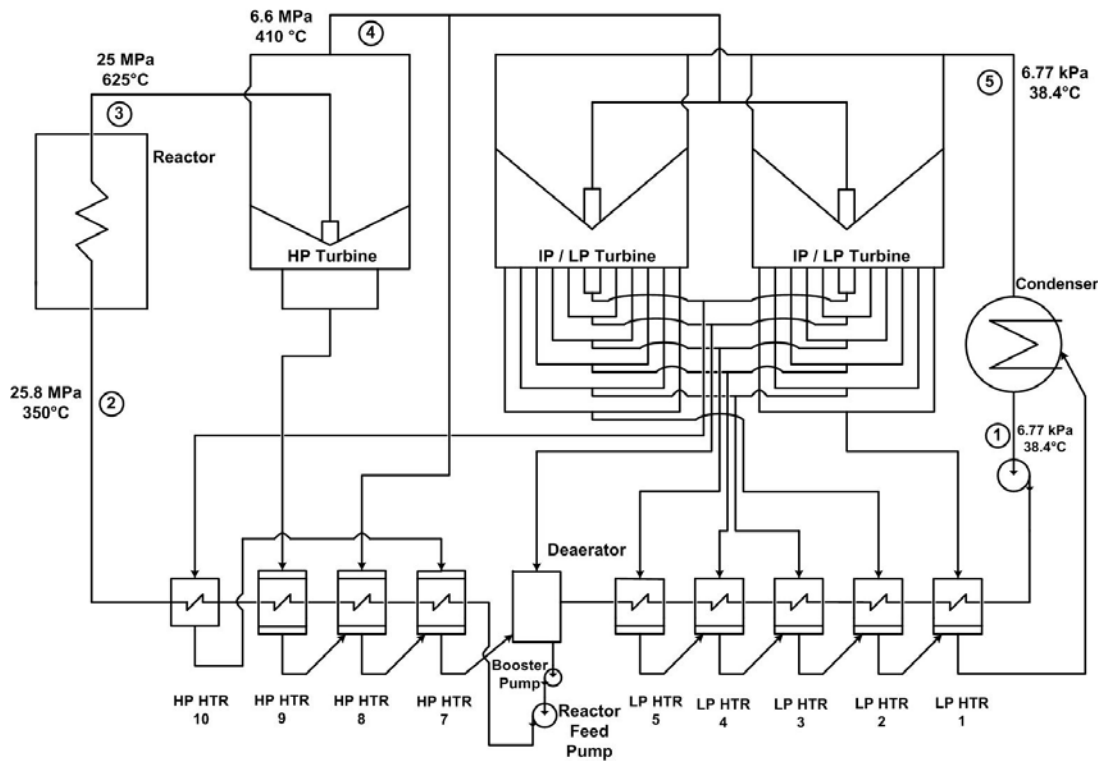


Fig. 4. No-Reheat Cycle D for SCW NPP [7].

#### 4. SCW NPP CYCLES ANALYSIS AND RESULTS

The T-s diagrams associated with the proposed SCW NPP cycles are illustrated in Figures 5–7, while thermal efficiencies for all three cycles are listed in Table 2.

For Cycle A (Figure 5) the exhausts of the HP and IP turbines remain in the superheated region, while those of the LP turbine fall into the saturated line. The calculated steam quality is approximately 87% at the condenser inlet.

In the case of Cycle B (containing the MSR unit), the exhaust of the HP turbine remains in the superheated region. However, the IP turbine exhaust falls under the saturation curve, having a steam quality of 98%. The MSR unit superheats the steam as shown in Figure 6, and the exhaust of the LP turbine is at saturated conditions with a steam quality of 86%.

Figure 7 shows the T-s diagram associated with the no-reheat SCW NPP Cycle C. The exhaust of the HP turbine is located in the superheated region, while that of the LP turbine falls in the saturated region. The moisture content at the outlet of the LP turbine is calculated to be 19%. This could be a major technical challenge for the SCW NPP based on the no-reheat cycle. However, the moisture can be reduced by implementing contoured channels in the inner casing for draining the water and moisture removal stages.

Table 2 lists values of thermal efficiency for the proposed SCW NPP single-reheat and no-reheat cycles. Table 3 illustrates the major parameters of the proposed thermal cycles, while Table 4 – PT SCWR major parameters.

Table 2. Thermal efficiency of SCW NPP Cycles.

| Cycle | Thermal Efficiency (%) |
|-------|------------------------|
| A     | 52                     |
| B     | 52                     |
| C     | 51                     |

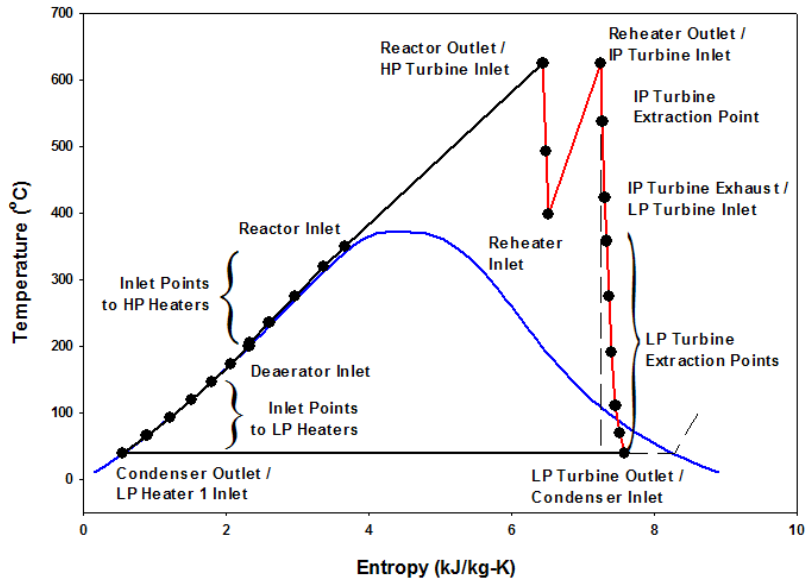


Fig. 5. T-s diagram for Single-Reheat Cycle A.

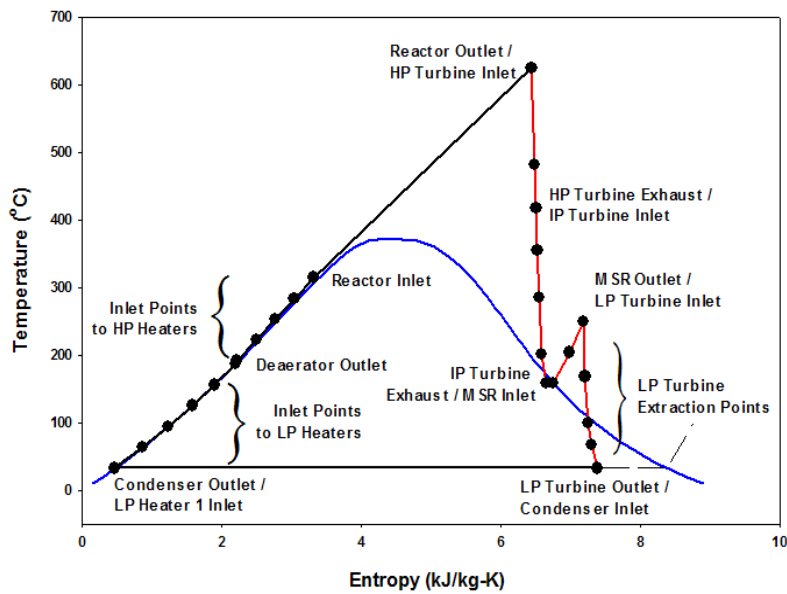


Fig. 6. T-s diagram for Single-Reheat Cycle C.



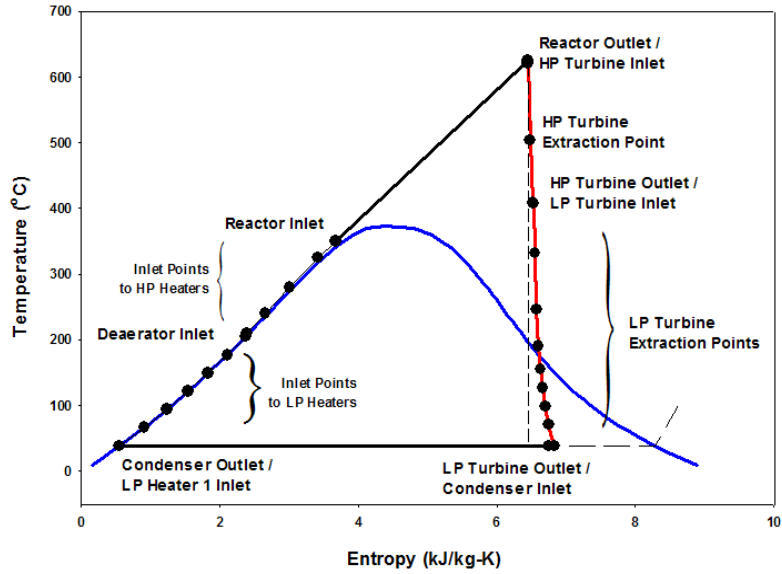


Fig. 7. T-s diagram for Single-Reheat Cycle C.

Table 3: Selected parameters of proposed SCW NPP Cycles A and C.

| Parameters                            | Unit             | Description / Value                 | Description / Value |
|---------------------------------------|------------------|-------------------------------------|---------------------|
| Cycle type                            | –                | Single-Reheat (A)                   | No-Reheat (C)       |
| Reactor type                          | –                | Pressure Tube                       |                     |
| Reactor spectrum                      | –                | Thermal                             |                     |
| Fuel                                  | –                | UO <sub>2</sub> (ThO <sub>2</sub> ) |                     |
| Cladding material                     | –                | Inconel or Stainless steel          |                     |
| Reactor coolant                       | –                | H <sub>2</sub> O                    |                     |
| Moderator                             | –                | D <sub>2</sub> O                    |                     |
| Power Thermal                         | MW <sub>th</sub> | 2300                                | 2340                |
| Power Electrical                      | MW <sub>el</sub> | 1200                                | 1200                |
| Thermal Efficiency                    | %                | 52                                  | 51                  |
| Pressure of SCW at inlet              | MPa              | 25.8                                | 25.8                |
| Pressure of SCW at outlet (estimated) | MPa              | 25                                  | 25                  |
| T <sub>in</sub> coolant (SCW)         | °C               | 350                                 | 350                 |
| T <sub>out</sub> coolant (SCW)        | °C               | 625                                 | 625                 |
| Pressure of SHS at inlet              | MPa              | 6.1                                 | –                   |
| Pressure of SHS at outlet (estimated) | MPa              | 5.7                                 | –                   |
| T <sub>in</sub> coolant (SHS)         | °C               | 400                                 | –                   |
| T <sub>out</sub> coolant (SHS)        | °C               | 625                                 | –                   |
| Power thermal SCW channels            | MW <sub>th</sub> | 1870                                | 2340                |
| Power thermal SRH channels            | MW <sub>th</sub> | 430                                 | –                   |
| Power thermal / SCW channel           | MW <sub>th</sub> | 8.5                                 | 8.5                 |
| Power thermal / SRH channel           | MW <sub>th</sub> | 5.5                                 | –                   |
| # of fuel channels (total)            | –                | 300                                 | 270                 |
| # of SCW channels                     | –                | 220                                 | 270                 |
| # of SRH channels                     | –                | 80                                  | –                   |
| Total flow rate of SCW                | kg/s             | 960                                 | 1190                |
| Total flow rate of SHS                | kg/s             | 780                                 | –                   |
| Flow rate / SCW channel               | kg/s             | 4.37                                | 4.37                |
| Flow rate / SRH channel               | kg/s             | 10                                  | –                   |

Table 4: Selected parameters of proposed SCWR fuel channels.

| Parameters  | Unit                | Description / Value  |            |            |
|---|---------------------|----------------------|------------|------------|
| $T_{\max}$ cladding (design value)  | °C                  | 850                  |            |            |
| $T_{\max}$ fuel centerline (industry accepted limit)                                      | °C                  | 1850                 |            |            |
| Heated fuel-channel length  | m                   | 5.772                |            |            |
| # of bundles / fuel channel   | –                   | 12                   |            |            |
| # of fuel rods per bundle   | –                   | 43                   |            |            |
| Bundle type [11]  | –                   | CANFLEX              | Variant-18 | Variant-20 |
| # of heated fuel rods   | –                   | 43                   | 42         | 42         |
| # of unheated* fuel rods  | –                   | –                    | 1          | 1          |
| Diameter of heated fuel rods (# of rods)  | mm                  | 11.5 (35) & 13.5 (8) | 11.5       | 11.5       |
| Diameter of unheated fuel rod   | mm                  | –                    | 18         | 20         |
| $D_{\text{hy}}$ of fuel channel   | mm                  | 7.52                 | 7.98       | 7.83       |
| $D_{\text{h}}$ of fuel channel  | mm                  | 9.04                 | 9.98       | 9.83       |
| Heated area of fuel channel   | m <sup>2</sup>      | 9.26                 | 8.76       | 8.76       |
| Flow area of fuel channel   | mm <sup>2</sup>     | 3625                 | 3788       | 3729       |
| Pressure tube inner diameter  | mm                  | 103.45               |            |            |
| <b>Average parameters of fuel channels in single-reheat (A) and no-reheat (B) options</b> |                     |                      |            |            |
| Heat flux in SCW channel (A&B cycles)   | kW/m <sup>2</sup>   | 918                  | 970        | 970        |
| Heat flux in SRH channel (A cycle)  | kW/m <sup>2</sup>   | 594                  | 628        | 628        |
| Mass flux in SCW channel (A&B cycles)   | kg/m <sup>2</sup> s | 1206                 | 1154       | 1172       |
| Mass flux in SRH channel (A cycle)  | kg/m <sup>2</sup> s | 2759                 | 2640       | 2682       |

## 5. SCWR FUEL-CHANNEL CALCULATIONS

SCWR technology is currently in its early design phase. A demonstration unit has yet to be designed and constructed. Fuel materials and configurations suited at supercritical conditions are currently being studied. This section describes thermal-design options of fuel bundles with respect to the maximum fuel centerline temperature to be restricted to 1850°C, and the maximum sheath temperature to be restricted to 850°C [4].

A model used in the current thermal-design analysis is a generic PT SCWR with 300 fuel channels and 1200-MW<sub>el</sub> power. A heated-channel length of 5.772 m is assumed. The anticipated fuel string consists of 12 bundles. Calculations consider the fuel-rod length to be equal to the heated-channel length, i.e., end-plates and end-caps of a bundle are not considered. Pressure drop along the channel was not accounted for, and pressure was assumed to be a constant 25 MPa. The contact resistance between a fuel pellet and sheath was considered to be negligible. Steady-state conditions with several uniform and cosine Axial Heat Flux Profiles (AHFPs) were applied. A coolant mass-flow rate per channel was assumed to be a constant 4.4 kg/s; and the produced power per channel – to be 8.5 MWth.

### 5.1 Background

Previous study [12] was performed to analyze different design features in SCW PT nuclear reactors. This study was performed using a generic 43-element fuel bundle with uranium fuel. However, this study considers only preliminary steady-state heat transfer coefficient (HTC) calculations, with a uniform AHFP and an average fuel thermal conductivity. This study has shown that the fuel centerline temperature might exceed the industry accepted limit of 1850°C for UO<sub>2</sub> fuel (see Figure 8). The same results were obtained in [13].

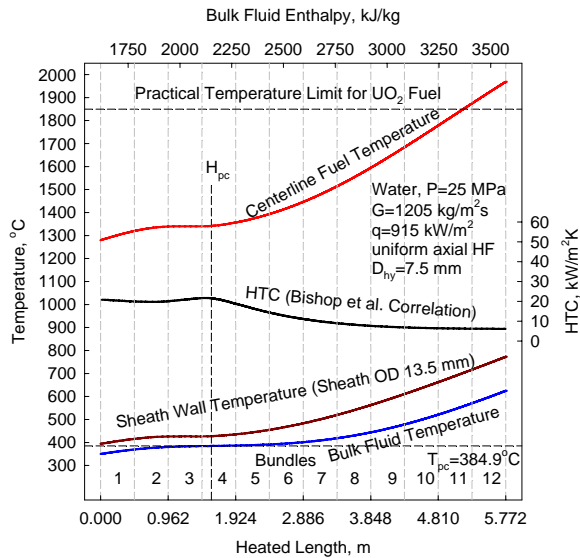


Fig. 8. Temperature and HTC profiles of  $UO_2$  along heated length of fuel channel (centreline fuel temperature based on average thermal conductivity of  $UO_2$ ) [12].

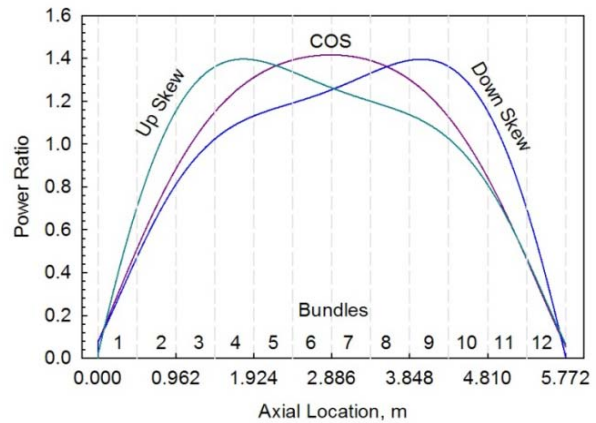


Fig. 9. Non-uniform AHFPs [11].

Therefore, the present section is dedicated to more representative nuclear-reactor AHFPs, such as cosine, upstream-skewed and downstream-skewed cosine profiles (for details, see Figure 9). The two fuel materials analyzed are UC and  $UC_2$  (UN fuel has thermal conductivity values in between those of UC and  $UC_2$  fuels), because these fuels have significantly higher thermal conductivities compared to those of  $UO_2$ , MOX and  $ThO_2$  materials.

## 5.2 Nuclear Fuels

The fuels compared in this paper are uranium dioxide ( $UO_2$ ), uranium carbide (UC) and uranium dicarbide ( $UC_2$ ). The main objective is to achieve a fuel composition with a lower fuel centerline temperature suited for the SCWR use. Uranium dioxide is commonly used in current reactors. However, it has a very low thermal conductivity that decreases as the temperature increases (for details, see Figure 10).

Therefore, new alternative nuclear fuels with higher thermal conductivities have to be considered. As shown in Figure 10, thermal conductivities of UC, UN and  $UC_2$  fuels are many times higher than that of conventional nuclear fuels such as  $UO_2$ , MOX and  $ThO_2$ ; and their thermal conductivities increase with increasing temperature. A fuel with a rising trend in thermal conductivity would increase heat transfer through a pellet and decrease fuel centreline temperature. This rising trend in thermal conductivity would be a key safety factor for SCWRs.

Table 5 lists important thermophysical properties of nuclear fuels. In general, there are many parameters such as density, porosity, method of manufacturing, etc., which might affect the thermal conductivity of any potential fuel [14]. Therefore, only generic thermal conductivities of nuclear fuels were used in the

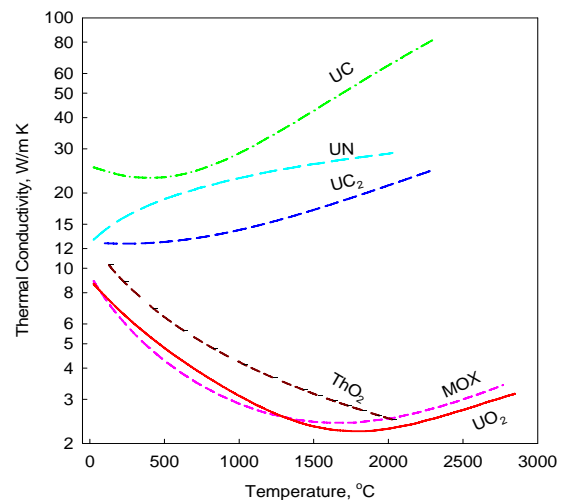


Fig. 10. Comparison of thermal conductivities of nuclear fuels [14] ([15] –  $UC_2$  and [16] –  $ThO_2$ ).

following calculations.

Table 5. Thermophysical properties of ceramic nuclear fuels at 0.1 MPa and 25°C [14] ([16] – ThO<sub>2</sub>).

| Property                        | Units             | Fuel                  |        |                      |                       |                       |                 |
|---------------------------------|-------------------|-----------------------|--------|----------------------|-----------------------|-----------------------|-----------------|
|                                 |                   | UO <sub>2</sub>       | MOX*   | ThO <sub>2</sub>     | UN                    | UC                    | UC <sub>2</sub> |
| Molar mass                      | kg/kmol           | 270.3                 | 271.2  | 264                  | 252                   | 250                   | 262             |
| Theoretical density             | kg/m <sup>3</sup> | 10,960                | 11,074 | 10,000               | 14,300                | 13,630                | 11,700          |
| Melting temperature             | °C                | 2850±30               | 2750   | 3227±150             | 2850±30               | 2365±165              | 2800±30         |
| Boiling temperature             | °C                | 3542                  | 3538   | >4227                | –                     | 4418                  | –               |
| Heat of fusion                  | kJ/kg             | 259±15                | 285.3  | –                    | –                     | 195.6                 | –               |
| Specific heat                   | kJ/kg·K           | 0.235                 | 0.240  | 0.235                | 0.190                 | 0.200                 | 0.162           |
| Thermal conductivity            | W/m·K             | 8.68                  | 7.82** | 9.7                  | 13.0                  | 25.3                  | 13              |
| Coefficient of linear expansion | 1/K               | 9.75·10 <sup>-6</sup> | –      | 8.9·10 <sup>-6</sup> | 7.52·10 <sup>-6</sup> | 10.1·10 <sup>-6</sup> | –               |

\* MOX – Mixed Oxides (U<sub>0.8</sub>Pu<sub>0.2</sub>) O<sub>2</sub>, where 0.8 and 0.2 are the molar parts of UO<sub>2</sub> and PuO<sub>2</sub>.

\*\* at 95% density.

### 5.3 Properties Profiles

Figure 11 shows thermophysical properties profiles (calculations based on NIST REFPROP software (2007)) of a light-water coolant along the heated-channel length for the downstream-skewed cosine AHFP. All thermophysical properties undergo significant and drastic changes within a pseudocritical region. This statement applies to all AHFPs. The only difference is the pseudocritical-point location along the bundle-string heated length, which depends on a particular AHFP (see also[13, 17]).

The average specific heat, average Prandtl number and density ratio (see Figure 12) were used in the Bishop et al. (1964) correlation [18].

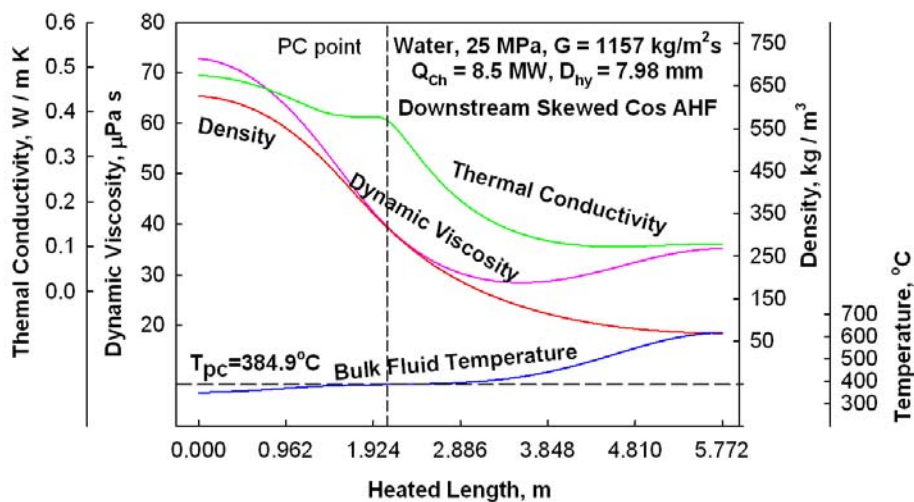


Fig. 11. Bulk-fluid temperature and thermophysical properties profiles along heated-bundle length at downstream-skewed AHFP.

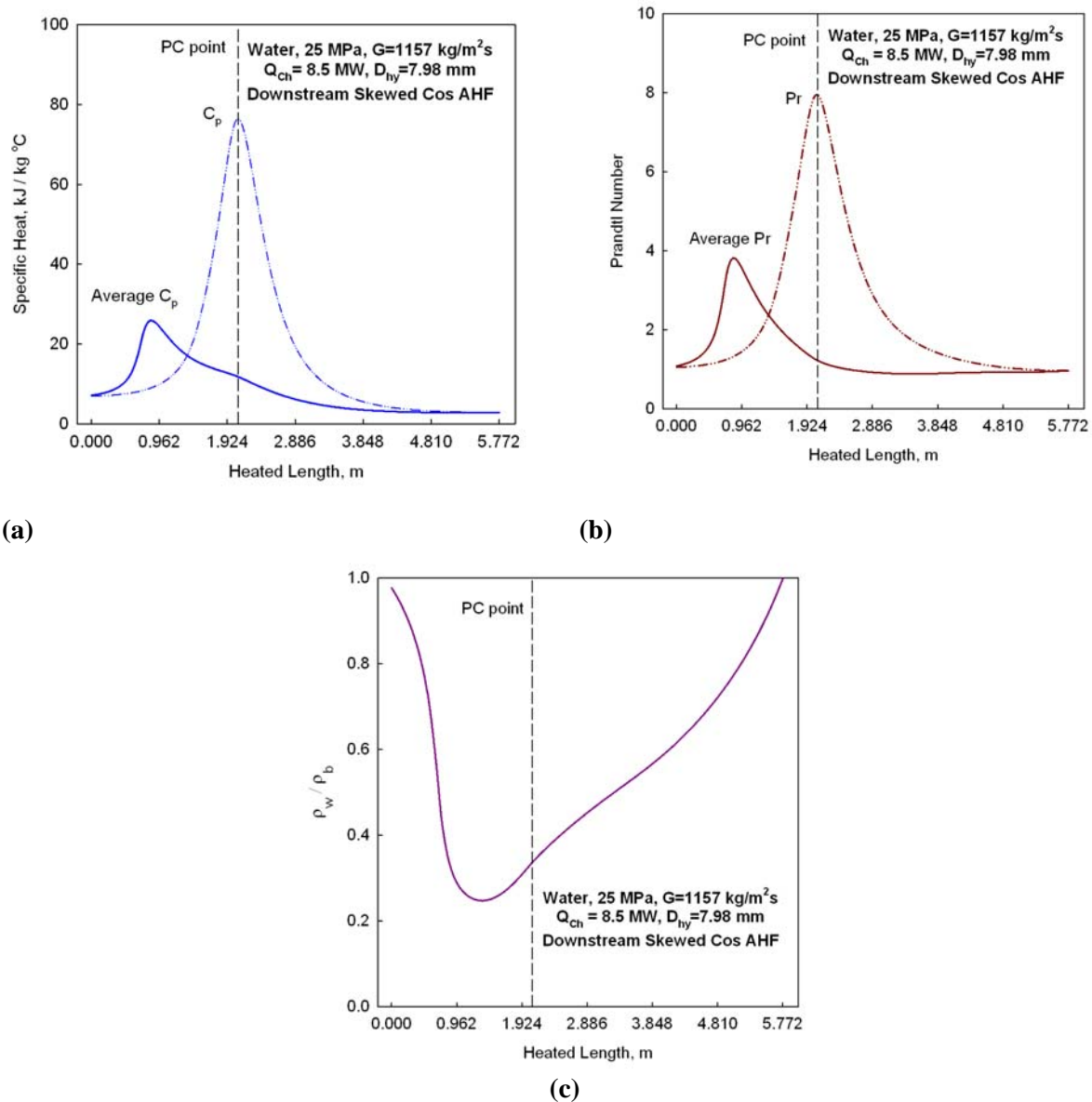


Fig. 12. Thermophysical properties profiles at downstream-skewed cosine AHFP: (a) “regular” and average specific heats, (b) “regular” and average Prandtl numbers and (c) density ratio.

#### 5.4 Methodology and Calculations

Thermophysical properties of the coolant at sheath temperature, and thermal conductivities of the sheath and fuel were calculated using an iterative method. In general, coolant properties were estimated based on a bulk-fluid temperature, i.e., an average coolant temperature in a cross section. All calculations were performed along the heated-bundle length with a 1-mm increment.

The bulk-fluid temperature was calculated through the heat-balance method. With the bulk-fluid temperature known and sheath temperature assumed, all properties can be determined at these temperatures, and using the Bishop et al. correlation the HTC can be calculated through iterations. The Bishop et al. correlation is suitable within a pressure range from 22.8 to 27.6 MPa, bulk-fluid temperatures between 282 and 527°C, and heat flux between 0.31 and 3.46 MW/m<sup>2</sup> [18]:

$$\text{Nu}_b = 0.0069 \text{Re}_b^{0.9} \text{Pr}_b^{0.66} \left( \frac{\rho_w}{\rho_b} \right)^{0.43} \left( 1 + 2.4 \frac{D}{x} \right) \quad (1)$$

The Bishop et al. correlation is applicable for tubes, and the last term represents the entrance effect in a bare tube. Accounting that fuel bundles have various appendages (endplates etc.) this term can be neglected. Also, it was assumed a perfect contact between a fuel pellet and sheath. The fuel centerline temperature was determined by small radial increments with variable thermal conductivity.

## 6. RESULTS

### 6.1 UO<sub>2</sub> Fuel Centerline Temperature

Uranium dioxide fuel centerline temperature surpasses the industry accepted limit of 1850°C at uniform (see Figure 7), cosine (see Figure 13a) and downstream-skewed cosine AHFPs (see Figure 13b).

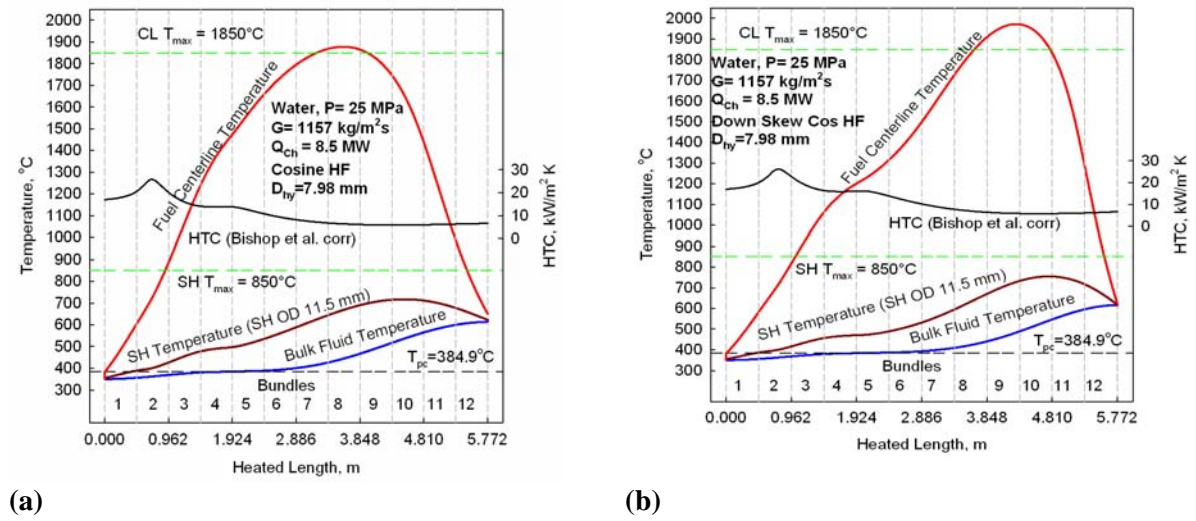


Fig. 13. Temperature and HTC profiles for UO<sub>2</sub> fuel: (a) at cosine AHFP and (b) at downstream-skewed AHFP.

### 6.2 UC and UC<sub>2</sub> Fuel Centerline Temperatures

Figure 14 shows variations in temperatures and HTC profiles along the heated-bundle length at non-uniform AHFPs for UC<sub>2</sub> fuel and Figure 15 – for UC fuel. An analysis of these graphs shows that all calculated cases with UC and UC<sub>2</sub> have significantly lower fuel centerline temperatures compared to those of UO<sub>2</sub> fuel at all uniform and non-uniform AHFPs due to their high thermal conductivity. The most desirable case in terms of the lowest fuel centerline temperature is UC fuel with the upstream cosine AHFP. In this case, the fuel centerline temperature does not exceed even the sheath-temperature design limit of 850°C.

However, with both UC and UC<sub>2</sub> fuels, there are factors beyond the scope of this paper in regards to porosity, density and manufacturing process, which must be accounted for when determining the feasibility of these substances as nuclear fuels for SCWRs.

## 7. NEW HEAT-TRANSFER CORRELATION FOR SUPERCRITICAL WATER FLOWING IN VERTICAL BARE CIRCULAR TUBES

This section presents a concise analysis of heat-transfer to supercritical water in bare vertical tubes (for more details, see [20–22]). A large set of experimental data obtained in Russia was analyzed, and a new heat-transfer correlation for supercritical water was developed. This experimental dataset was obtained within conditions similar to those in SCWR concepts.

The experimental dataset was obtained in supercritical water flowing upward in 4-m long vertical bare tube with 10-mm ID. The data were collected at pressures of about 24 MPa, inlet temperatures from 320 to 350°C, values of mass flux ranged from 200 – 1500 kg/m<sup>2</sup>s and heat fluxes up to 1250 kW/m<sup>2</sup> for several combinations of wall and bulk-fluid temperatures that were below, at, or above the pseudocritical temperature.

A dimensional analysis was conducted using the Buckingham *Π*-theorem to derive a general form of empirical supercritical water heat-transfer correlation for the Nusselt number, which was finalized based on the experimental data obtained at the normal heat-transfer regime (please see below). Also, experimental HTC values at the normal heat-transfer regime were compared with those calculated according to several correlations from the open literature, CFD code and those of the derived correlation.

A comparison [20] (see Figure 16) showed that the Dittus-Boelter correlation significantly overestimates experimental HTC values within the pseudocritical range. The Bishop et al. and Jackson correlations tended also to deviate substantially from the experimental data within the pseudocritical range. The Swenson et al. correlation provided a better fit for the experimental data than the previous three correlations within some flow conditions, but does not follow up closely the experimental data within others. Also, HTC and wall temperature values calculated with the FLUENT CFD code [23] might deviate significantly from the experimental data, for example, the *k-ε* model (wall function). However, the *k-ε* model (low *Re* numbers) shows better fit within some flow conditions.

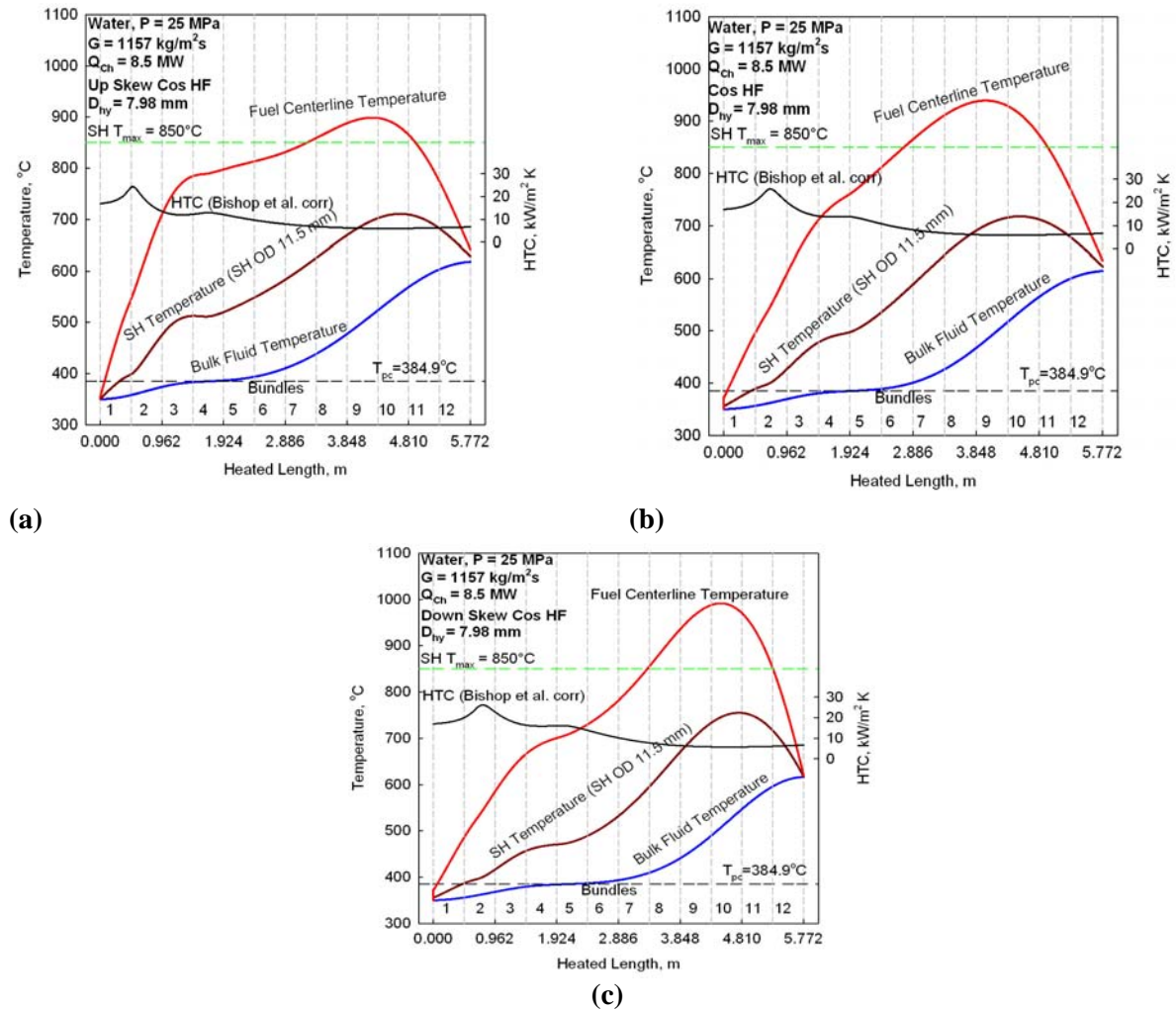
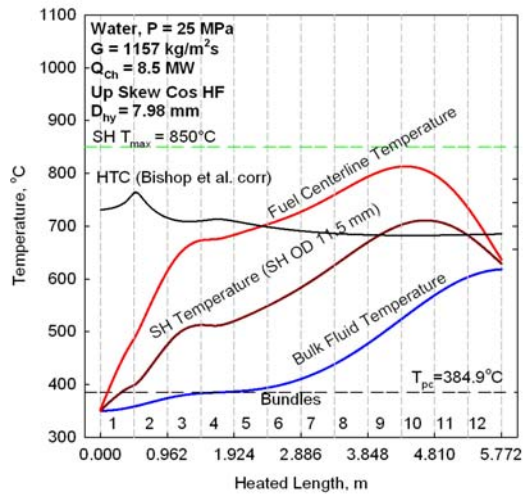
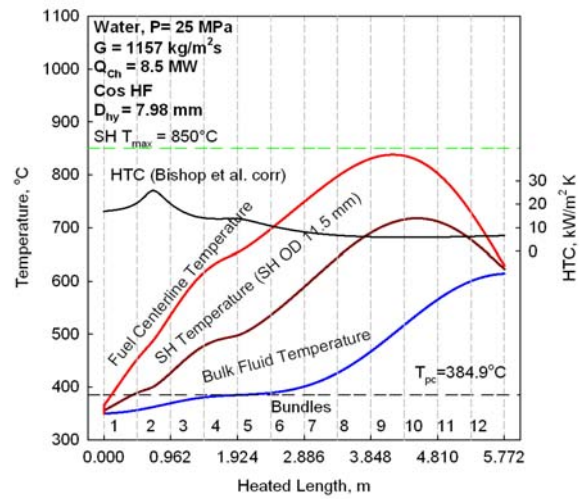


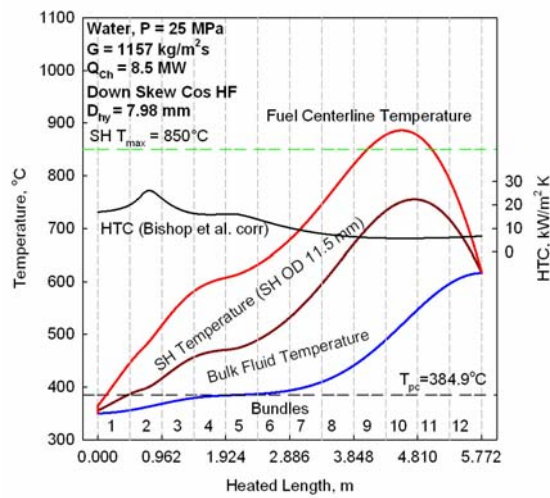
Fig. 14. Temperature and HTC profiles along heated length of fuel channel for UC<sub>2</sub> fuel: (a) at upstream-skewed cosine AHFP, (b) at cosine AHFP and (c) at downstream-skewed cosine AHFP.



(a)



(b)



(c)

Fig. 15. Temperature and HTC profiles along heated length of fuel channel for UC fuel [19]: (a) at upstream-skewed cosine AHFP, (b) at cosine AHFP and (c) at downstream-skewed cosine AHFP.



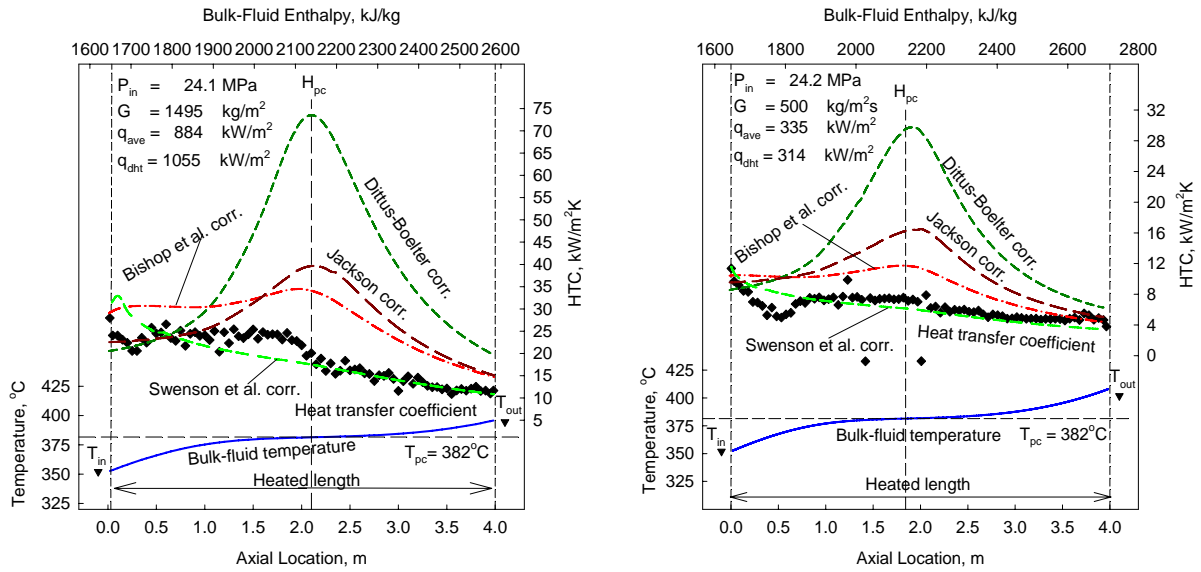


Fig. 16. Comparison of HTC values calculated with various correlations from open literature with experimental data along 4-m circular tube ( $D=10$  mm):  $P_{in}=24.0$  MPa and  $G=1500$  and  $500$   $\text{kg/m}^2\text{s}$ .

Nevertheless, the derived correlation

$$\text{Nu}_b = 0.0061 \text{Re}_b^{0.904} \text{Pr}^{0.684} \left( \frac{\rho_w}{\rho_b} \right)^{0.564} \quad (2)$$

showed the best fit for the experimental data within a wide range of flow conditions (see Figures 17 and 18). This correlation has uncertainty of about  $\pm 25\%$  for HTC values and about  $\pm 15\%$  for calculated wall temperature (see Figure 19).

Therefore, the derived correlation can be used for HTC calculations of SCW heat exchangers, for preliminary HTC calculations in SCWR fuel bundles, for future comparison with other datasets, for verification of computer codes and scaling parameters between water and modeling fluids.

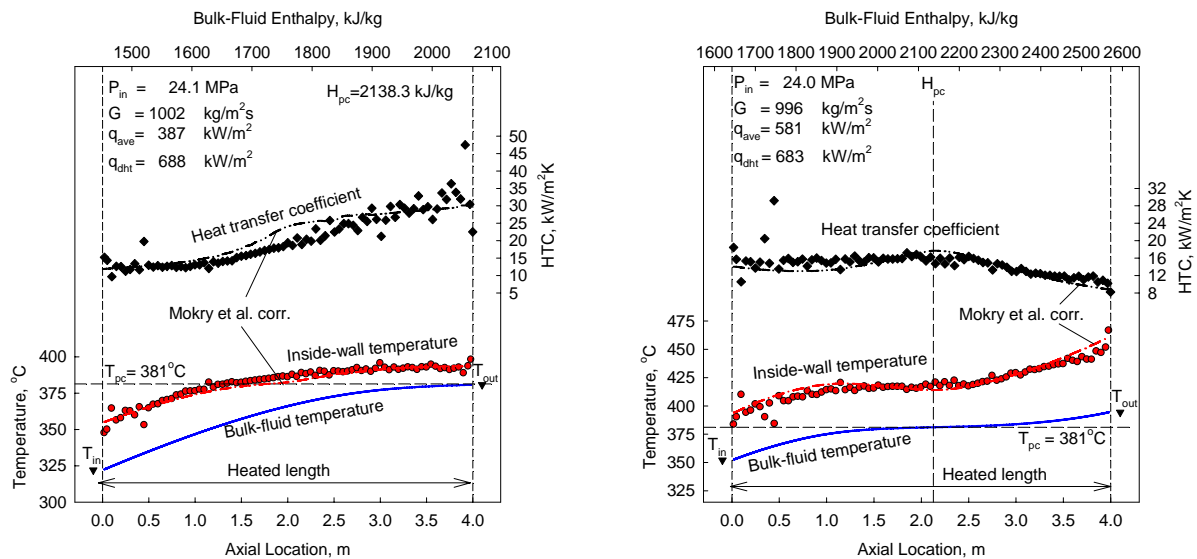


Fig. 17. Temperature and HTC variations at various heat fluxes along 4-m circular tube ( $D=10$  mm; Mokry et al. correlation is Eq. (2)):  $P_{in}=24.0$  MPa and  $G=1000$   $\text{kg/m}^2\text{s}$ .

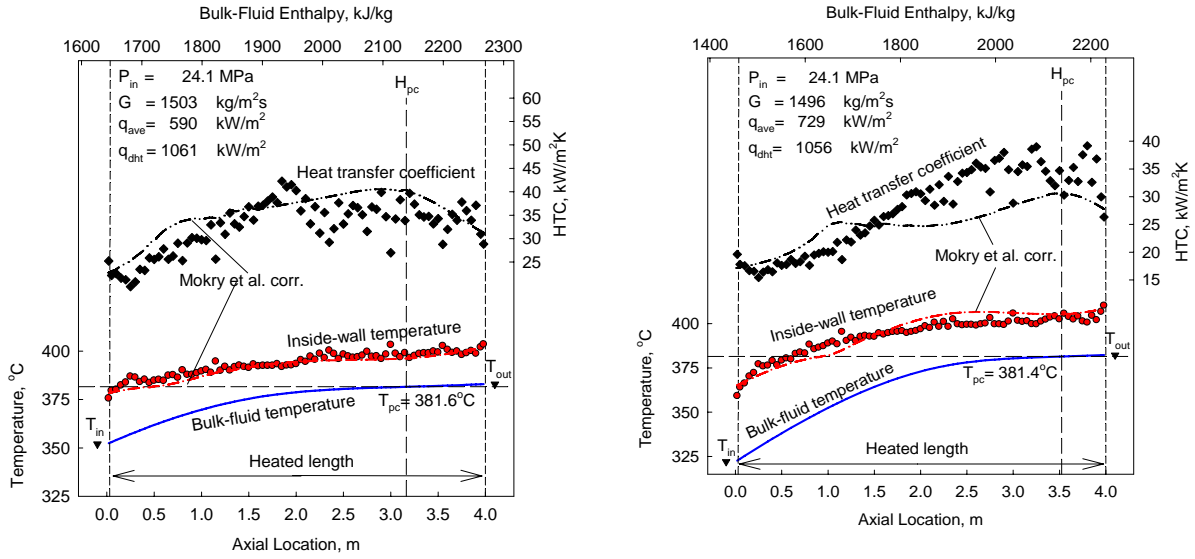


Fig. 18. Temperature and HTC variations at various heat fluxes along 4-m circular tube ( $D=10$  mm; Mokry et al. correlation is Eq. (2)):  $P_{in}=24.0$  MPa and  $G=1500$  kg/m<sup>2</sup>s.

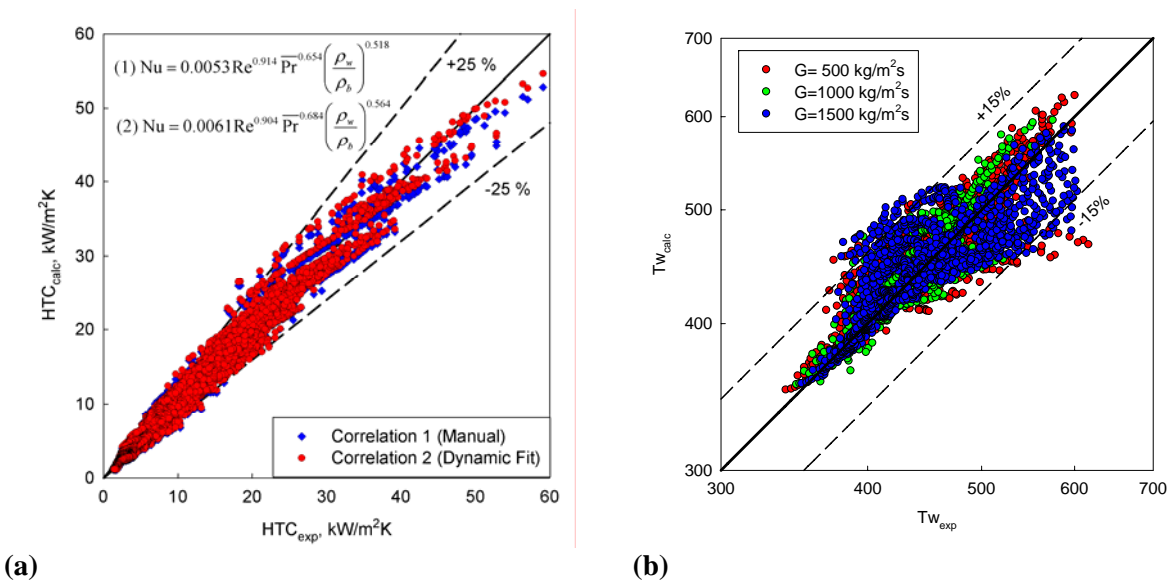


Fig. 19. Comparison of data fit with experimental data: (a) for HTC and (b) for  $T_w$ .

## CONCLUSIONS

The following conclusions can be made:

- The vast majority of the modern SC turbines are single-reheat-cycle turbines. Just a few double-reheat-cycle SC turbines have been manufactured and put into operation. However, despite their efficiency benefit double-reheat-turbines have not been considered economical.
- Major inlet parameters of the current and upcoming single-reheat-cycle SC turbines are: the main or primary SC “steam” – pressure of 24 – 25 MPa and temperature of 540 – 600°C; and the reheat or secondary subcritical-pressure steam –  $P = 3 - 5$  MPa and  $T = 540 - 620^\circ\text{C}$ .
- Usually, inlet temperatures of the main SC “steam” and the reheat subcritical-pressure steam are the same or very close (for example, 566/566°C; 579/579°C; 600/600°C; 566/593°C; 600/620°C).

- In order to maximize the thermal-cycle efficiency of the SCW NPPs it would be beneficial to include nuclear steam reheat. Advantages of a single-reheat cycle in application to SCW NPPs are:
  - High thermal efficiency (45 – 50%), which is the current level for SC thermal power plants and close to the maximum thermal efficiency achieved in the power industry at combined-cycle power plants (up to 55%).
  - High reliability through proven state-of-the-art turbine technology; and
  - Reduced development costs accounting on wide variety of SC turbines manufactured by companies worldwide.
- The major disadvantage of a single-reheat cycle implementation in SCW NPPs is the requirement for significant changes to the reactor-core design due to addition of the nuclear steam-reheat channels at subcritical pressures.
- Based on the abovementioned analysis, the single-reheat cycle with heat regeneration and the corresponding arrangement appear to be the most advantageous as a basis for a SCW NPP with the co-generation of hydrogen.
- In general, UO<sub>2</sub> nuclear fuel might not be a good choice for SCWRs, because at certain conditions the fuel centerline temperature exceeds the industry accepted limit of 1850°C.
- UC, UN and UC<sub>2</sub> nuclear fuels with significantly higher thermal conductivities might be considered as alternative fuels compared to conventional fuels such as UO<sub>2</sub>, MOX and ThO<sub>2</sub>. These fuels can be used at any AHFPs: cosine, upstream-skewed or downstream-skewed cosine. However, further investigation would be required into properties of UC, UN and UC<sub>2</sub> as they are new fuels.
- UC nuclear fuel with its highest thermal conductivity values compared to that of other nuclear fuels (UO<sub>2</sub>, MOX, ThO<sub>2</sub>, UN and UC<sub>2</sub>) will have the largest safety margin for the fuel centerline temperature.
- The following supercritical-water heat-transfer dataset obtained in a vertical bare tube was used for development of a new heat-transfer correlation and its comparison with the experimental data, with other correlations from the open literature and with FLUENT CFD code:  $P=24$  MPa,  $T_{in} = 320 - 350^{\circ}\text{C}$ ,  $G = 200 - 1500$  kg/m<sup>2</sup>s and  $q \leq 1250$  kW/m<sup>2</sup>. This dataset was obtained within the SCWR operating conditions.
- The comparison showed that the Dittus-Boelter correlation significantly overestimates experimental HTC values within the pseudocritical range. The Bishop et al. and Jackson correlations tended also to deviate substantially from the experimental data within the pseudocritical range. The Swenson et al. correlation provided a better fit for the experimental data than the previous three correlations within some flow conditions, but does not follow up closely the experimental data within others. Also, HTC and wall temperature values calculated with the FLUENT CFD code might deviate significantly from the experimental data (for example, the  $k-\varepsilon$  model (wall function)). However, the  $k-\varepsilon$  model (low Reynolds numbers) shows better fit within some flow conditions.
- Nevertheless, the derived correlation showed the best fit for the experimental data within a wide range of flow conditions. This correlation has uncertainty about  $\pm 25\%$  for HTC values and about  $\pm 15\%$  for calculated wall temperature.
- Therefore, the derived correlation can be used for HTC calculations of SCW heat exchangers, for preliminary HTC calculations in SCWR fuel bundles, for future comparison with other datasets, for verification of computer codes and scaling parameters between water and modeling fluids.

## ACKNOWLEDGEMENTS

Financial supports from the NSERC Discovery Grant, NSERC/NRCan/AECL Generation IV Energy Technologies Program and Ontario Research Excellence Fund are gratefully acknowledged.

## NOMENCLATURE

|             |   |
|-------------|---|
| $c_p$       | specific heat at constant pressure, J/kg·K                                |
| $\bar{c}_p$ | average specific heat, J/kg·K, $\left(\frac{H_w - H_b}{T_w - T_b}\right)$ |
| $D$         | diameter, m   |
| $G$         | mass flux, kg/m <sup>2</sup> s  |
| $H$         | enthalpy, J/kg  |
| $h$         | heat transfer coefficient, W/m <sup>2</sup> K                             |
| $k$         | thermal conductivity, W/m·K   |
| $P$         | pressure, Pa  |
| $Q$         | heat-transfer rate, W   |
| $q$         | heat flux, W/m <sup>2</sup>   |
| $s$         | entropy, J/kg K   |
| $T$         | temperature, °C   |

Greek letters

|        |                            |
|--------|----------------------------|
| $\mu$  | dynamic viscosity, Pa·s    |
| $\rho$ | density, kg/m <sup>3</sup> |

Dimensionless numbers

|                   |   |
|-------------------|---|
| <b>Nu</b>         | Nusselt number $\left(\frac{h \cdot D}{k}\right)$                   |
| <b>Pr</b>         | Prandtl number $\left(\frac{\mu \cdot c_p}{k}\right)$               |
| $\bar{\text{Pr}}$ | average Prandtl number $\left(\frac{\mu \cdot \bar{c}_p}{k}\right)$ |
| <b>Re</b>         | Reynolds number $\left(\frac{G \cdot D}{\mu}\right)$                |

Subscripts

|      |            |
|------|------------|
| b    | bulk       |
| calc | calculated |
| ch   | channel    |

|     |                            |
|-----|----------------------------|
| dht | deteriorated heat-transfer |
| el  | elctrical                  |
| exp | experimental               |
| hy  | hydraulic                  |
| in  | inlet                      |
| pc  | pseudocritical             |
| th  | thermal                    |
| w   | wall                       |

Abbreviations:

|         |                             |
|---------|-----------------------------|
| AHFP    | Axial Heat Flux Profile     |
| BWR     | Boiling Water Reactor       |
| CANDU   | CANada Deuterium Uranium    |
| CANFLEX | CANDU FLEXible (fuelling)   |
| CEP     | Condensate Extraction Pump  |
| HHV     | Higher Heating Value        |
| HP      | High Pressure               |
| HTC     | Heat Transfer Coefficient   |
| HTR     | Heater                      |
| HWR     | Heavy Water Reactor         |
| IP      | Intermediary Pressure       |
| LP      | Low Pressure                |
| LWR     | Light-Water Reactor         |
| ID      | Inside Diameter             |
| MOX     | Mixed Oxide                 |
| MSR     | Moisture Separator Reheater |
| NPP     | Nuclear Power Plant         |
| PC      | PseudoCritical              |
| PT      | Pressure Tube (reactor)     |
| PV      | Pressure Vessel (reactor)   |
| PWR     | Pressurized Water Reactor   |
| RFP     | Reactor Feedwater Pump      |
| SC      | SuperCritical               |
| SCW     | SuperCritical Water         |
| SCWR    | SuperCritical Water Reactor |
| SH      | Sheath                      |
| SHS     | SuperHeated Steam           |
| SRH     | Steam ReHeat                |

**REFERENCES**

- [1] Piroo, I. & Duffey, R., 2007. Heat Transfer and Hydraulic Resistance at Supercritical Pressures in Power Engineering Applications, ASME Press, New York, NY, USA, 334 pages.
- [2] Naterer, G., Suppiah, S., Lewis, M., et al., 2009. Recent Canadian Advances in Nuclear-Based Hydrogen Production and the Thermochemical Cu-Cl Cycle, Int. J. of Hydrogen Energy, Vol. 34, Issue 6, 17 pages.
- [3] Naidin M., Piroo I., Zirn, U., Mokry S. and Naterer, G., 2009. Supercritical Water-Cooled NPPs with Co-Generation of Hydrogen: General Layout and Thermodynamic-Cycles Options, Proc. 4<sup>th</sup> Int. Symp. on Supercritical Water-Cooled Reactors, March 8-11, Heidelberg, Germany, Paper No. 78, 11 pages.

- [4] Chow, C. K. and Khartabil, H.F., 2008. Conceptual Fuel Channel Designs for CANDU-SCWR. *Nuclear Engineering and Technology*, Vol. 40, No. 1, pp. 1–8.
- [5] Duffey, R.B., Pioro, I., Zhou, T., Zirn, U., Kuran, S., Khartabil, H. and Naidin, M., 2008. Supercritical Water-Cooled Nuclear Reactors (SCWRs): Current and Future Concepts - Steam-Cycle Options, Proc. ICONE-16, Orlando, Florida, USA, May 11-15, Paper #48869, 9 pages.
- [6] Duffey, R.B., Pioro, I.L. and Kuran, S., 2008. Advanced Concepts for Pressure-Channel Reactors: Modularity, Performance and Safety, *JSME J. of Power and Energy Systems*, Vol. 2, No. 1, 10 pages.
- [7] Naidin, M., Monichan, R., Zirn, U., Gabriel, K. and Pioro, I., 2009. Thermodynamic Considerations for a Single-Reheat Cycle SCWR, Proc. ICONE-17, July 12-16, Brussels, Belgium, Paper #75984, 8 pages.
- [8] Naidin, M., Pioro, I., Duffey, R., Zirn, U. and Mokry, S., 2009. SCW NPPs: Layouts and Thermodynamic Cycles Options, Int. Conf. “Nuclear Energy for New Europe”, Bled, Slovenia, Sep. 14-17.
- [9] Naidin, M., Pioro, I., Zirn, U. and Chophla, K., 2009. SuperCritical Water Reactor NPP Concept: No-Reheat Cycle Option, Proc. ICONE-17, July 12-16, Brussels, Belgium, Paper #75989, 9 pages.
- [10] Naidin, M., Mokry, S., Baig, F., Gospodinov, Ye., 2008. Thermal-Design Options for Pressure-Channel SCWRs with Cogeneration of Hydrogen, *J. of Eng. for Gas Turbines and Power*, Vol.131, Issue 1, Paper #012901, 8 pages.
- [11] Leung, L., 2008. Effect of CANDU Bundle-Geometry Variation on Dryout Power, Proc. ICONE-16, Orlando, Florida, USA, May 11-15, Paper #48827, 8 pages.
- [12] Pioro, I., Khan, M., Hopps, V., Jacobs, C., Patkunam, R., Gopaul, S., and Bakan, K., 2008. SCW Pressure-Channel Nuclear Reactor Some Design Features, *J. of Power and Energy Systems*, pp. 874-888.
- [13] Allison, L., Villamere, B., Grande, L., Mikhael, S., Rodriguez-Prado, A. and Pioro, I., 2009. Thermal Design Options for SCWR Fuel Channel with Uranium Carbide and Uranium Di-Carbide Ceramic Fuels, Proc. ICONE-17, July 12-16, Brussels, Belgium, Paper #75975, 10 pages.
- [14] Kirillov, P.L., Terent'eva, M.I. and Deniskina, N.B., 2007. *Thermophysical Properties of Nuclear Engineering Materials*, 2<sup>nd</sup> ed. revised and augmented), Izdat Publ. House, Moscow, Russia, 194 pages.
- [15] Chirkin, V.S., 1968. *Thermophysical Properties of Materials for Nuclear Engineering*, (In Russian), Atomizdat Publ. House, Moscow, Russia.
- [16] Jain, D., Pillai, C., Rao, B. K., & Sahoo, K., 2006. Thermal Diffusivity and Thermal Conductivity of Thoria-Lanthana Solid Solutions up to 10 mol.% LaO(1.5). *J. of Nuclear Materials*, pp. 35-41.
- [17] Grande, L., Villamere, B., Rodriguez-Prado, A., Mikhael, S., Allison, L. and Pioro, I., 2009. Thermal Aspects of Using Thoria Fuel in Supercritical Water-Cooled Nuclear Reactors, Proc. ICONE-17, Brussels, Belgium, July 12-16, Paper #75969, 10 pages.

- [18] Bishop, A., Sandberg, R. & Tong, L., 1964. Forced Convection Heat Transfer to Water at Near-Critical Temperatures and Super-Critical Pressures, Report WCAP, Westinghouse Electric Corporation, Atomic Power Division, Pittsburgh, PA, USA, December, 106 pages.
- [19] Villamere, B., Grande, L., Rodriguez-Prado, A., Mikhael, S., Allison, L. and Pioro, I., 2009. Thermal Aspects for Uranium Carbide and Uranium Dicarbide Fuels in Supercritical Water-Cooled Nuclear Reactors, Proc. ICONE-17, July 12-16, Brussels, Belgium, Paper #75990, 10 pages.
- [20] Mokry, S., Farah, A., King, K., Gupta, S., Pioro, I. and Kirillov, P., 2009. Development of a Supercritical Water Heat-Transfer Correlation for Vertical Bare Tubes, Int. Conf. "Nuclear Energy for New Europe", Bled, Slovenia, Sep. 14-17.
- [21] Mokry, S., Gospodinov, Ye., Pioro, I. and Kirillov, P.L., 2009. Supercritical Water Heat-Transfer Correlation for Vertical Bare Tubes, Proc. ICONE-17, July 12-16, Brussels, Belgium, Paper #76010, 8 pages.
- [22] Pioro, I.L., Kirillov, P.L., Mokry, S.J. and Gospodinov, Y.K., 2008. Supercritical Water Heat Transfer in a Vertical Bare Tube: Normal, Improved and Deteriorated Regimes, Proc. ICAPP-08, Anaheim, CA, USA, June 8-12, Paper #8333, pp. 1843-1852.
- [23] Vanyukova, G.V., Kuznetsov, Yu.N., Loninov, A.Ya., Papandin, M.V., Smirnov, V.P. and Pioro, I.L., 2009. Application of CFD-Code to Calculations of Heat Transfer in a Fuel Bundle of SCW Pressure-Channel Reactor, Proc. 4<sup>th</sup> Int. Symp. on Supercritical Water-Cooled Reactors, March 8-11, Heidelberg, Germany, Paper No. 28, 9 pages.